# Intense Sub-Kilometer-Scale Boundary Layer Rolls Observed in Hurricane Fran

Joshua Wurman* and Jennifer Winslow

High-resolution observations obtained with the Doppler On Wheels (DOW) mobile weather radar near the point of landfall of hurricane Fran (1996) revealed the existence of intense, sub-kilometer-scale, boundary layer rolls that strongly modulated the near-surface wind speed. It is proposed that these structures are one cause of geographically varying surface damage patterns that have been observed after some landfalling hurricanes and that they cause much of the observed gustiness, bringing high-velocity air from aloft to the lowest observable levels. High-resolution DOW radar observations are contrasted with lower-resolution observations obtained with an operational weather radar, which underestimated peak low-level wind speeds.

Small-scale variations in damage patterns have been observed in surveys after hurricane landfalls in the United States and in Japan (*1*, *2*). Human-made structures and trees in damage swaths may experience major damage or total destruction, whereas those outside are only lightly affected. These damage patterns can exhibit strong periodicity with scales near 500 m and may contain scales as small as 10 to 200 m. It is unlikely that these sub-kilometer-scale features are caused by typical thunderstorm-like structures, because the latter are typically >5 km in scale in landfalling hurricanes (*3*, *4*). It has been speculated that convective elements in hurricane rain bands and in the eye wall intensify, possibly as a consequence of increased surface friction and convergence, causing localized regions of more damaging winds. Small-scale damage may occur as a result of microbursts, mesoscale vortices, or tornadoes spawned by these intensified elements (*1*, *2*, *5*–*7*). However, direct observational evidence of the cause of these small-scale damage patterns has been scarce. Here, we present high-resolution (20 to 200 m) Doppler weather radar observations of the rain bands and eye wall of hurricane Fran as it made landfall near Wilmington, North Carolina, during the evening of 5 September 1996 [near midnight 05/06 September 1996 UTC (Coordinated Universal Time)]. The data were obtained with a mobile pulsed Doppler weather radar, the DOW (*8*–*10*).

The DOW radar was driven from Norman, Oklahoma to the South Carolina coast in anticipation of the landfall of hurricane Fran (*11*). After adjusting for changes in the storm's forecast path, the radar was deployed at New Hanover International Airport in Wilmington (ILM) on an aircraft taxiway closed for this purpose (*12*). The airport is ~10 km from the coastline and 50 km from the National Weather Service radar southeast of Wilmington (call letters, KLTX) (Fig. 1) and was directly in the path of the eye of Fran as it crossed the North Carolina coastline. The large eye of the hurricane, moving almost due north along longitude 78°W, crossed the coastline of North Carolina during the period 0000 to 0200 UTC, with the center of the eye making landfall at ~0030 UTC. Airborne radar observations indicated winds of 55 to 58 m $s^{-1}$ at altitudes above 3000 m before and at landfall. Surface observations indicated peak winds of more than 55 m $s^{-1}$ at the coast near the point of landfall. Winds at the airport gusted to near 40 m $s^{-1}$ at the National Weather Service station and to ~45 m $s^{-1}$ on an uncalibrated anemometer mounted on the DOW radar truck (*13*, *14*). Radar reflectivity data from the KLTX radar near the time of landfall (Fig. 2) show the large eye surrounded by an eye wall and intense rain bands. Convective elements ~10 km in scale (*3*, *4*) are visible to the north of the radar. As the storm neared landfall, the eye structure disintegrated so that the rear of the eye became indistinct. Data were collected by the DOW from 2030 UTC 05 September 1997 until 0210 UTC 06 September 1997, covering the period leading up to and immediately after landfall.

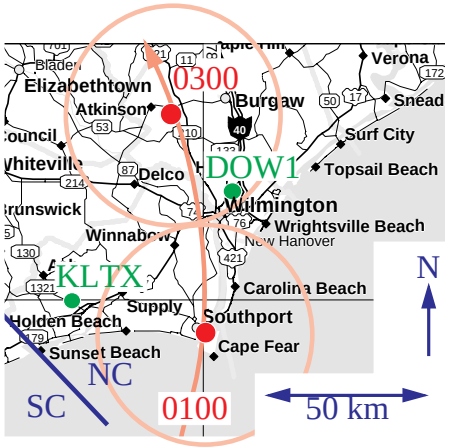


**Fig. 1.** Radar locations and approximate hurricane Fran eye path near Wilmington, North Carolina, from 0100 to 0300 UTC 06 September 1996.

Before landfall, the large-scale flow pattern well above the ground exhibited the expected intense, 50 to 60 m $s^{-1}$, onshore flow (Fig. 3) (*15*), veering ~40° between 0 m and 1000 m agl (above ground level); however, below 500 m agl, the wind field contained striking small-scale spatial variations (Fig. 4). These variations were in the form of bands of intense winds (40 to 60 m $s^{-1}$) alternating with much weaker flow (15 to 35 m $s^{-1}$). The bands were oriented approximately parallel to the larger scale flow, with a cross-wind wavelength (peak to peak) of ~600 m (highly variable), and were aligned approximately parallel to the 0 to 1000 m agl wind shear vector, crossing the 100 to 1000 m agl shear vector at ~30°.

We propose that the bands of alternating high and low wind speeds were the signature of axially horizontal rolls superimposed on the larger scale flow pattern (Fig. 5). Air moving at ~60 m $s^{-1}$ at 1000 m agl was transported toward the surface in the downward legs of the rolls, while air slowed by frictional and turbulent drag at and near the ground was transported aloft in the upward legs. Thus, the horizontal velocity of air in

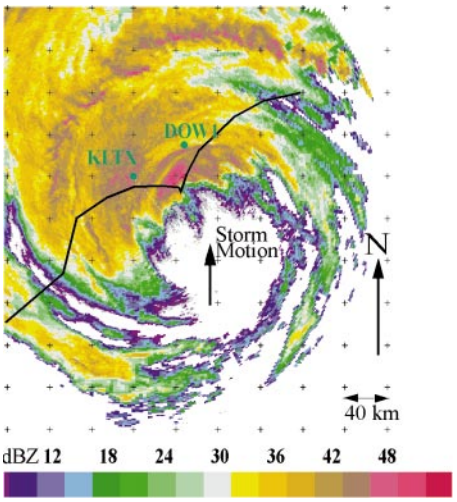


**Fig. 2.** Large-scale radar reflectivity (dBZ) structure of the eye and surrounding rain bands in hurricane Fran as it made landfall on the North Carolina coast at 2327 UTC 05 September 1996, as measured by the KLTX National Weather Service WSR-88D radar. Rain bands surrounding the large eye and structures within the rain bands, particularly to the north and northwest of the eye, contain features with ~10-km scale. Scan is at 0.5° elevation (*17*).

School of Meteorology, University of Oklahoma, 100 East Boyd Street, Norman, OK 73019, USA.

*To whom correspondence should be addressed. E-mail: jwurman@ou.edu

the downdrafts approached the 55 to 60 m $s^{-1}$ values typical of 1000 to 1300 m agl, whereas air in the updrafts originated near the ground, where wind speeds had been reduced to ~20 to 30 m $s^{-1}$. The efficiency of the rolls in transporting potentially damaging horizontal momentum to the ground is illustrated in Fig. 6, where DOW-measured peak horizontal wind speeds are shown to be homogenized throughout the lowest 2000 m agl. DOW-measured peak wind speeds of 55 m $s^{-1}$ near the coastline at 50 to 100 m agl, and 40 to 45 m $s^{-1}$ below 50 m agl near the airport, were very close to those observed by surface instrumentation. The roll perturbations resulted in horizontal wind shear as high as 30 m $s^{-1}$ over 300 m, corresponding to a vertical component of shear vorticity of up to 0.1 $s^{-1}$. These values are as high as those observed at similar resolution in weak tornadoes, but not in strong ones (*8*). The velocity associated with the cross-roll flow (perpendicular to the large-scale horizontal flow) was estimated to be 3 to 5 m $s^{-1}$ by measuring the Doppler velocity in regions where the radar beams were oriented perpendicular to the rolls.

Radar volumes were updated every 300 s; these intervals were too long to permit estimation of roll propagation velocity or of the scan-to-scan evolution of stronger wind field perturbation features embedded within the rolls (Fig. 4). Time scales associated with these smaller perturbations might be as short as the size of the perturbations (100 to 300 m) divided by the average wind speed (40 m $s^{-1}$), or 2.5 to 8 s. However, the spatial scale and magnitude of the features suggest that they are associated with much of the gustiness observed in hurricanes at landfall. Close to the radar, below 50 m agl and at the finest resolution, DOW-observed perturbations (~20 m $s^{-1}$) from the mean flow (35 to 40 m $s^{-1}$) correspond to gust factors of ~1.5, close to those observed by anemometers in hurricanes (*16*). Small-scale boundary layer rolls, providing efficient and focused transport of horizontal momentum from 1000 m agl to the surface, may be the cause of some small-scale variations in damage. However, some damage surveys (*1*, *2*) have documented damage swaths much smaller than the wavelength of the rolls. These damage swaths may be attributable to sub-roll-scale maxima suggested by the DOW data.

Boundary layer rolls have long been observed in convectively unstable environments in the presence of vertical shear of the horizontal wind, and have been described theoretically, computationally, and in the laboratory (*17*–*27*). Because rolls parallel to the wind shear vector are only expected in environments that are convectively unstable, the orientation of the observed rolls implies that the lowest 1000 m of the hurricane was at least slightly convectively unstable in the landfall region despite nighttime conditions, heavy prelandfall rainfall, and persistent cloudiness during the day before landfall. Direct observation of the thermal structure of the overland hurricane boundary layer with conventional balloon measurements is, of course, problematic. An alternate possibility is that the banded structure is the result of hairpin vortices observed in the laboratory and described theoretically (*28*, *29*). Extremely long hairpin vortices might be observationally indistinguishable from horizontal rolls because radar beams may miss the sharp-turning sections of the hairpins.

Horizontal winds were observed to weaken after the hurricane eye passed over the radar site after 0100 UTC. The rolls were absent in the region of weaker flow in the disintegrating hurricane eye, but they persisted inland, where winds of 50 m $s^{-1}$ continued at 1000 m agl, suggesting that a threshold wind speed may have been necessary for the observed roll instability to be manifested or that the environment may have become more convectively stable within the eye.

Data from the nearby KLTX radar were

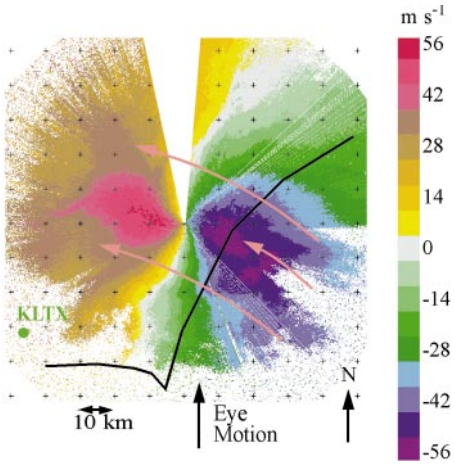


**Fig. 3.** Large-scale Doppler velocity structure at 23:30:19 UTC, as measured by the DOW radar. Strong easterly flow peaking at ~60 m $s^{-1}$ is evident both off- and onshore. The eye of the hurricane is at the edge of radar visibility to the south. Visibility was severely limited by attenuation. Pink curved arrows illustrate average wind flow. Scan is at 5° elevation.

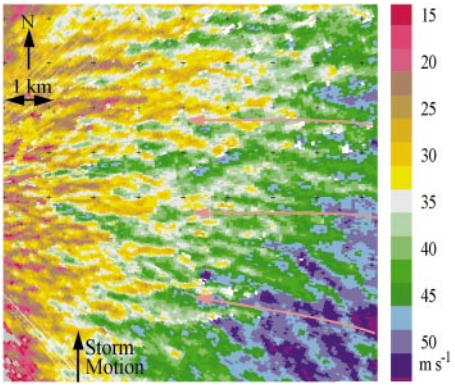


**Fig. 4.** High-resolution image of Doppler velocity field to the east of Wilmington at 23:58:17 UTC. Sub-kilometer-scale streaks caused by boundary layer rolls modulate the mean easterly flow. Near the radar (left) at altitudes of ~100 m agl, peak and trough wind speed values are ~40 m $s^{-1}$ and ~10 m $s^{-1}$, respectively. Further from the radar (right), peak and trough wind speed values alternate from ~25 to ~55 m $s^{-1}$. Azimuthal shear values are (~30 m $s^{-1}$/~300 m) ≈ 0.1 $s^{-1}$ across many of the rolls. Scan is at 2° elevation.

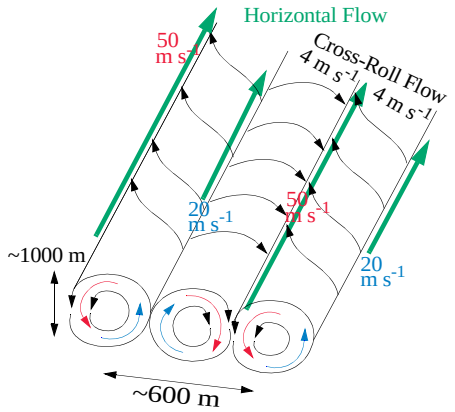


**Fig. 5.** Schematic representation of observed shear- and wind-parallel boundary layer rolls. High-momentum air (red) is brought to the surface in the downward legs of the rolls, while air slowed near the surface is brought aloft in the upward legs.

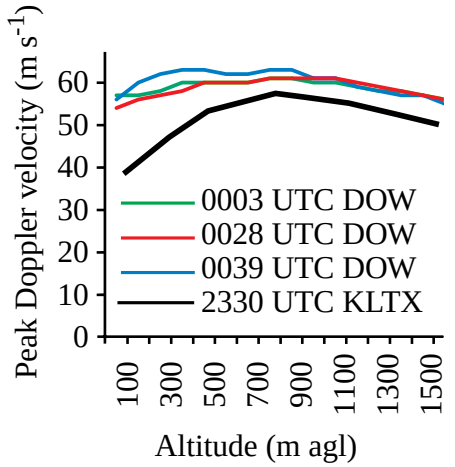


**Fig. 6.** Altitude dependence of peak wind speeds as observed by DOW and National Weather Service KLTX radars. DOW-measured peak speeds at 100 m agl are nearly as high as those at 1000 m agl as a result of momentum transport in the rolls and agree closely with surface peak wind observations. KLTX-measured peak speeds are smaller at low altitude because of poorer resolution and possibly because of longer overland trajectories.

reported at coarser range resolution than the DOW data: 75 m for the DOW, 250 m for KLTX. Furthermore, the DOW oversampled azimuthally, calculating four beams per degree, whereas KLTX collected only one beam per degree. KLTX resolution was thus coarser than that of the DOW by a factor of 3.5 to 7. Because the roll wavelength was ~600 m with sub-roll peak wind speed regions with scales of ~100 m (Fig. 4), the rolls were less accurately characterized by KLTX and the peak wind intensity was underestimated. Peak-to-trough differences in wind speeds were near 10 m $s^{-1}$, only 30% of that observed by the DOW and lower than typical hurricane gust factors (*16*). An important consequence was that the KLTX data implied less severe peak low-level wind speeds than were observed at the ground or by the DOW (Fig. 6). Because the wind field sampled near KLTX had passed over ~40 km of land, some of the observed differences likely resulted from evolution of the near-surface wind field.

### REFERENCES AND NOTES


1. R. Wakimoto and P. Black, *Bull. Am. Meteorol. Soc.* **75**, 189 (1994).
2. T. T. Fujita, *Storm Data* **34**, 25 (1992).
3. D. Jorgensen, *J. Atmos. Sci.* **41**, 1268 (1984).
4. _____, *ibid*., p. 1287.
5. M. S. Powell, S. Houston, T. Reinhold, *Weather Forecast.* **11**, 329 (1996).
6. F. Marks Jr. and R. Houze Jr., *Bull. Am. Meteorol. Soc.* **65**, 569 (1984).
7. S. Stewart, J. Simpson, D. Wolff, in *22nd Conference on Hurricanes and Tropical Meteorology* (American Meteorological Society, Boston, 1997), p. 106.
8. J. Wurman, J. M. Straka, E. N. Rasmussen, *Science* **272**, 1774 (1996).
9. _____, M. Randall, A. Zahrai, *J. Atmos. Ocean. Tech.* **14**, 1502 (1997).
10. The DOW1 radar prototype described in (*9*) was upgraded to include a 2.44-m antenna, improved signal processing, and other hardware and software. The radar used a 40-kW transmitter operating at 9.375 GHz (32 mm). Pulses were 450 ns in duration, repeating every 500 μs, and sampled every 500 ns, resulting in range resolution of 75 m. The 2.44-m parabolic antenna produced a 0.95° beam, which spread to a width of 160 m at a range of 10 km from the radar. Radar beams were oversampled, resulting in 4 beams per degree.
11. This data collection mission was coordinated with the Hurricane Research Division (HRD) of the National Oceanic and Atmospheric Administration. F. Marks and S. Houston of HRD provided forecast guidance, other information, and coordination with the local weather service forecast office in Wilmington, NC. M. Biddle and C. Edwards, with J.W., crewed the DOW radar.
12. The Wilmington Weather Service Forecast Office provided real-time forecasting guidance and logistical support during the data collection. New Hanover International Airport provided the data site, logistics, and safety coordination during data collection. The taxiway was well removed from sources of airborne debris, particularly trees, tree limbs, and portions of damaged buildings. The tree line was generally 400 to 1000 m distant and blocked only the lowest radar beams, which were less than 1° above the horizon. The airport terminal building caused blockage up to several degrees above the horizon in the southern sector. Wetting of the antenna cover caused severe attenuation of both transmitted and received radiation, reducing sensitivity by 10 to 20 dB during periods of intense rainfall. Reflectivity and Doppler velocity data were collected in eight conical scans with inclinations ranging from 0° to 30° above the horizon, repeating every 300 s, to sample the volume of space surrounding the radar.
13. P. Dodge, S. Houston, J. Gamache, in (*7*), p. 115.
14. S. Houston, M. Powell, P. Dodge, *ibid*., p. 92.
15. Data were translated, plotted, displayed, and gridded by the NCAR programs xltrs, solo, reorder, and zeb, partially described in R. Oye and R. Carbone, in *20th Conference on Radar Meteorology* (American Meteorological Society, Boston, 1981), p. 683.
16. W. R. Krayer and R. D. Marshall, *Bull. Am. Meteorol. Soc.* **73**, 613 (1992).
17. T. Weckwerth, J. Wilson, R. Wakimoto, *Mon. Weather Rev.* **124**, 769 (1996).
18. T. Weckwerth, J. Wilson, R. Wakimoto, N. Crook, *ibid*. **125**, 505 (1997).
19. K. E. Emanuel, *Atmospheric Convection* (Oxford Univ. Press, New York, 1994).
20. T. Asai, *J. Meteorol. Soc. Jpn.* **48**, 18 (1970).
21. _____, *ibid*. **50**, 525 (1972).
22. J. Kuettner, *Tellus* **23**, 404 (1971).
23. M. LeMone, *J. Atmos. Sci.* **30**, 1077 (1973).
24. A. Faller, *ibid*. **23**, 466 (1965).
25. W. Sun, *ibid*. **35**, 466 (1978).
26. R. Sykes and D. Henn, *ibid*. **46**, 1106 (1989).
27. R. Kropfli and N. Kohn, *J. Appl. Meteorol.* **17**, 669 (1978).
28. J. Kim and R. Moser, *J. Fluid Mech.* **177**, 133 (1987).
29. S. Kline, W. Reynolds, F. Schraub, P. Runstadler, *ibid*. **30**, 741 (1967).


30. Supported by the Cooperative Institute for Mesoscale Meteorological Studies and the School of Meteorology at the University of Oklahoma. The DOW radars are a collaborative effort among the University of Oklahoma, the National Center for Atmospheric Research, and the National Severe Storms Laboratory.

30 December 1997; accepted 19 February 1998


# Switching Supramolecular Polymeric Materials with Multiple Length Scales


J. Ruokolainen, R. Mäkinen, M. Torkkeli, T. Mäkelä, R. Serimaa, G. ten Brinke,* O. Ikkala*



It was demonstrated that polymeric supramolecular nanostructures with several length scales allow straightforward tailoring of hierarchical order-disorder and order-order transitions and the concurrent switching of functional properties. Poly(4-vinyl pyridine) (P4VP) was stoichiometrically protonated with methane sulfonic acid (MSA) to form $P4VP(MSA)_{1.0}$, which was then hydrogen-bonded to pentadecylphenol. Microphase separation, re-entrant closed-loop macrophase separation, and high-temperature macrophase separation were observed. When MSA and pentadecylphenol were complexed to the P4VP block of a microphase-separated diblock copolymer poly[styrene-*block*-(4-vinyl pyridine)], self-organized structures-in-structures were obtained whose hierarchical phase transitions can be controlled systematically. This microstructural control on two different length scales (in the present case, at 48 and 350 angstroms) was then used to introduce temperature-dependent transitions in electrical conductivity.


During the past decade, methods to prepare nanosized structures have progressed greatly, stimulated by the continuing demand for miniaturization of devices and electronic components. Polymers offer a means to construct ordered nanoscale domains through self-organization, on the basis of competing interactions (*1*–*7*). Perhaps the most studied example is provided by block copolymers, where the repulsion between the chemically connected blocks leads to self-organization into lamellar, cylindrical, spherical, and other structures with length scales on the order of 100 to 1000 Å (*1*). Even more complicated structures have been created with block copolymers containing rigid moieties (*4*, *8*). Recently, another concept to achieve mesomorphic structures at much smaller length scales (typically 30 to 40 Å) has been presented in which nonmesogenic amphiphilic oligomers are noncovalently bonded to homopolymers (*5*, *6*, *9*). In the case of hydrogen bonding between amphiphilic oligomers such as pentadecylphenol (PDP) and homopolymers such as P4VP, the competition between attraction and repulsion leads to a microphase-separated (often lamellar) morphology at low temperatures (*6*, *10*, *11*). Heating yields an order-disorder transition to a disordered phase (*10*, *11*).

Here, we show that the two above-mentioned ordering principles can be combined with the use of diblock copolymers consisting of a coil-like block and a block consisting of a supramolecular polymer-amphiphile complex, allowing microstructural control on two length scales. The hierarchi-


J. Ruokolainen and O. Ikkala, Department of Engineering Physics and Mathematics, Helsinki University of Technology, FIN-02015 HUT, Espoo, Finland.
R. Mäkinen, M. Torkkeli, R. Serimaa, Department of Physics, University of Helsinki, Post Office Box 9, FIN-00014, Helsinki, Finland.
T. Mäkelä, VTT Microelectronics, Technical Research Centre of Finland, Post Office Box 1101, FIN-02044 VTT, Espoo, Finland.
G. ten Brinke, Department of Polymer Science and Materials Science Center, University of Groningen, Nijenborgh 4, 9747 AG Groningen, Netherlands.

*To whom correspondence should be addressed. E-mail: G.ten.Brinke@chem.rug.nl; Olli.Ikkala@hut.fi